Available online at www.sciencedirect.com
SCIENCE DIRECT®
ELSEVIER
Journal of Magnetism and Magnetic Materials 262 (2003) 15–22
Journal of magnetism and magnetic materials
www.elsevier.com/locate/jmmm

Giant Hall effect in superparamagnetic granular films

J.C. Denardin[a,b], M. Knobel[a,*], X.X. Zhang[b], A.B. Pakhomov[c]

[a] *Instituto de Física "Gleb Wataghin" (IFGW), Universidade Estadual de Campinas (UNICAMP), C.P. 6165, Campinas S.P. 13083-970, Brazil*

[b] *Physics Department and Institute of Nanoscience and Technology (INST), Hong Kong University of Science and Technology, Clear Water Bay, Kowloon, Hong Kong, China*

[c] *Department of Materials Science, University of Washington, Seattle, WA 98195, USA*

Abstract

A comprehensive review of the giant Hall effect (GHE) is presented, with emphasis on novel experimental data obtained in Ni–SiO_2 and Co–SiO_2 films prepared by co-sputtering. GHE is observed close to and on both sides of the metal–insulator transition. From the point of view of microscopic conduction mechanisms, this means a crossover from metallic conductivity with weak localization to tunneling, or hopping, between separate granules across insulating barriers. Magnetic percolation is also interrupted at this concentration of metal, leading to superparamagnetic behavior of the composite and blocking phenomena. Temperature dependencies of magnetization and extraordinary Hall coefficient in the composites near the critical concentration are compared. In single phase magnetic metals and alloys, the extraordinary Hall is believed to be directly proportional to the total magnetization, due to side jumps or skew scattering. In a metal–insulator composite, only those electrons traveling in conduction critical paths can contribute to the Hall signal, thus only magnetization of the material belonging to these paths is important in the Hall measurements. Comparison with the magnetic results leads to new possibilities in understanding both the electronic and magnetic properties of granular nanocomposites.

Keywords: Giant Hall effect; Granular systems; Magnetic nanoparticles; Spin-dependent electronic transport

1. Introduction

Transport, magnetoresistance, magnetic, dielectric and optical properties of both magnetic and non-magnetic granular metals, or cermets, have been studied since late 1960s [1]. However, transport close to the metal–insulator transition (MIT) remains not fully understood. Most commonly, in co-sputtered composites, one can distinguish between metallic conduction, characterized by a positive temperature coefficient of resistivity (TCR) at high metal concentrations (above a critical concentration x_c), and activated tunneling (or hopping) for concentrations below x_c. In the latter case, the resistance follows a law with $R \cong R_0 \exp[(T_0/T)^n]$, where n most often $\sim\frac{1}{2}$ due to variable range hopping with a wide distribution of charging energies [2]. A mechanism in the vicinity of x_c, leading to a logaritmic dependence of resistance ($R \propto -\log T$) up to room temperature, is often attributed to weak localization in a connected disordered metal

*Corresponding author. Tel.: +55-19-3788-5480; fax: +55-19-3289-3137.

E-mail address: knobel@ifi.unicamp.br (M. Knobel).

0304-8853/03/$ - see front matter
doi:10.1016/S0304-8853(03)00012-X

network [2]. However, the $R \propto -\log T$ dependence can be also associated with tunneling, that occurs in a disconnected network [3]. Tunneling magnetoresistance (TMR) in magnetic cermets near the MIT has been known since 1972 [4], and it has been intensively studied recently [5,6].

Giant Hall effect (GHE) is another remarkable property of granular systems discovered in 1995 [7]. GHE was first observed in cermets where the metallic component was ferromagnetic. It was found that near the critical concentration of metal in the composite (x_c) for the MIT, in the region where $R \propto -\log T$, the extraordinary Hall resistivity can be a factor up to 10^4 larger than that in the pure metal (NiFe, for example) [7].

In non-magnetic metals, the Hall coefficient is originated from the Lorentz force, and it is rather small, owing to the high charge carrier density. However, in bulk magnetic metals or metals with magnetic impurities, there are two contributions to the Hall effect, one originated from the Lorentz force, the so-called ordinary Hall resistivity ($\rho_{xyo} = R_0 B$) and the other originated from spin–orbit interaction (skew scattering and/or side jump mechanisms) [8], the extraordinary Hall resistivity ($\rho_{xy}^M = R_s 4\pi M$). The extraordinary Hall effect (EHE) is usually much larger (~ 10 times) than the ordinary one, and the curves of Hall vs. field resemble magnetization curves [8].

Complete theoretical interpretations of GHE in granular composites were hindered by considerable problems. Classical percolation theory predicts a divergence of the Hall effect at the percolation threshold in three dimensions, but the observed GHE is much greater than the estimate of this theory for finite sample thickness [9]. Therefore, other possibilities have been proposed, but the choice of the theoretical model strongly relies on the experimental determination of the type of conductance in the vicinity of the critical concentration.

In this work, a brief review of the GHE is presented, with emphasis on novel experimental data obtained in Co–SiO_2 and Ni–SiO_2 films prepared by co-sputtering. GHE is clearly correlated with the nanostructure (investigated by means of transmission electron microscopy (TEM) and other techniques) of granular samples near the MIT. Also, examples of the use of Hall measurements as a tool to investigate granular superparamagnetic systems are presented and discussed.

2. GHE: experimental examples

The 500 nm thick granular $Co_x(SiO_2)_{1-x}$, $Ni_x(SiO_2)_{1-x}$ and Co_xAg_{1-x} films with different magnetic volume fractions x were prepared in a magnetron co-sputtering system, with the transition metal and SiO_2 (or Ag) targets mounted on two separate guns. The glass substrates were rotated during sputtering, to ensure composition uniformity. The metal volume fraction was controlled by the relative sputtering rates, and then determined by energy-dispersive X-ray spectroscopy using a Philips EDAX XL30 on films deposited in the same run on Kapton. The samples deposited on Kapton were used for magnetic measurements. Structural characterization was performed by TEM using a Jeol JEM-3010 ARP microscope, and by X-ray diffractometry. Magnetization and transport properties were measured in the Quantum Design MPMS XL7 system in the temperature range 5–300 K and fields up to 7 T. Resistance and magnetoresistance were measured in bar-shaped samples using the four-probe method. The samples used for Hall measurements were prepared with masks in the usual double-cross geometry. Further details of microstructural characterization are given elsewhere [10].

The dominant type of conductance in the samples was initially determined from the analysis of the temperature dependence of resistivity shown in Fig. 1(a) for $Co_x(SiO_2)_{1-x}$ and in Fig. 1(b) for $Ni_x(SiO_2)_{1-x}$, where the temperature is displayed on a logarithmic scale. The samples with high values of x behave as typical metals with impurities. For the other samples the TCR at low T is negative. In samples with values between $0.6 < x < 0.85$, TCR is positive at high temperatures, and a minimum of R is observed, which shifts towards higher temperatures with decreasing metal concentration. For the samples with $x \sim 0.52$, in the case of $Co_x(SiO_2)_{1-x}$, and $x \sim 0.57$, in the case of $Ni_x(SiO_2)_{1-x}$, the dependence is

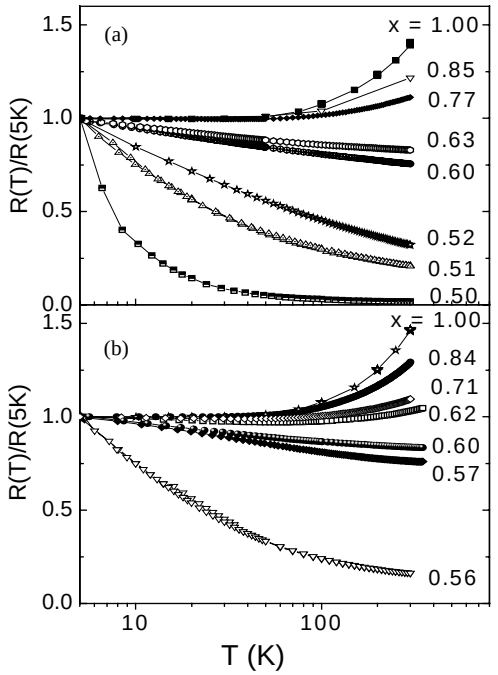

Fig. 1. Resistivity, normalized to the values at $T = 5\,\mathrm{K}$, as a function of the logarithm of temperature for (a) $Co_x(SiO_2)_{1-x}$ and (b) $Ni_x(SiO_2)_{1-x}$ samples with different metal volume fraction x.

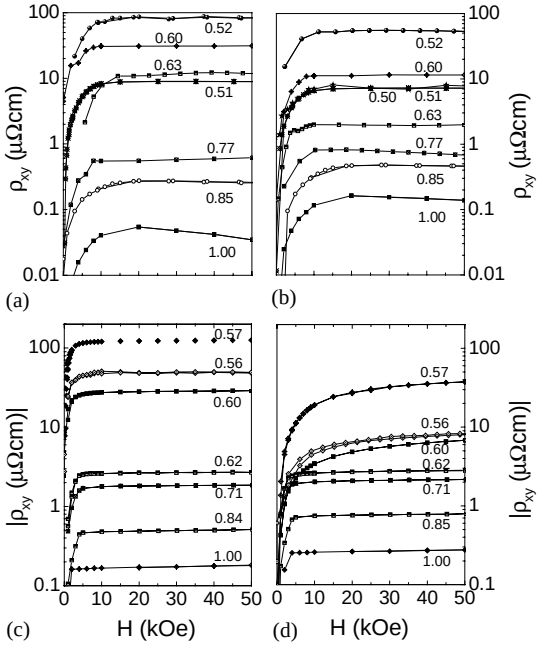

Fig. 2. Hall resistivity, in a logarithmic scale, as a function of magnetic field for $Co_x(SiO_2)_{1-x}$ [(a) 5 K; (b) 300 K] and $Ni_x(SiO_2)_{1-x}$ [(c) 5 K; (d) 300 K] samples with different x.

approximately logarithmic, $\rho \propto -\log T$, with negative TCR in the whole scanned temperature range. It is worth noting that similar temperature dependencies of resistivity have been observed in other co-sputtered metal–insulator materials with varying x [7,9], fact that reflects similarities in microstructure. The $\rho \propto -\log T$ dependence has been attributed to weak localization or electron–electron interaction effects in a disordered metallic system. However, a recent study shows that it can be a signature of the dominating tunneling conduction with large localization length [3]. For samples with lower x the temperature dependence of R is stronger than $-\log T$, and can be well described by an exp $[(T_0/T)^n]$ law ($n \sim 0.4$) for $Co_{0.5}[SiO_2]_{0.5}$ sample, that is a signature of hopping or tunneling. Figs. 2(a) and (b) show the Hall resistivity of the $Co_x(SiO_2)_{1-x}$ samples as a function of magnetic field at $T = 5$ and 300 K (note that the scale of y-axis is logarithmic). Magnetization curves for these samples (not shown here) are well saturated for fields above 2 T (at 5 K). Hence, the saturation extraordinary Hall resistivity ρ_{xys} can be determined by the linear extrapolation of the saturated part of the ρ_{xy} vs. H curves, i.e., from above 2 T to zero field. On the other hand, the ordinary Hall resistivity ρ_{xyo} can be roughly estimated from the slopes at fields larger than 2 T. In all Co samples the ordinary Hall effect is negative, while the extraordinary one is positive, analogous to pure metallic cobalt [8]. Both components of the Hall effect are enhanced with decreasing metal volume fraction, both at low and high temperatures. Figs. 2(c) and (d) show the Hall resistivity of the $Ni_x(SiO_2)_{1-x}$ system for the same temperatures. In these samples both ordinary and EHE are negative (the absolute values are shown in the figure).

The choice of composites containing cobalt helps one to unambiguously separate the two contributions to the Hall effect, because they display different signs. We found that the enhancement of the ordinary Hall effect is considerably smaller than that of the extraordinary part.

The ratio of the values of ρ_{xyo} in the sample with $x = 0.52$ (for Co–SiO_2), and $x = 0.57$ (for Ni–SiO_2), to ρ_{xyo} in samples with $x = 1.00$ can be used to characterize the enhancement of the ordinary Hall effect as the system undergoes the MIT. On the other hand, for the extraordinary effect one can use the corresponding ratio of the values of ρ_{xys}. At $T = 5\,K$, the value of ρ_{xyo} increased from $-6.5 \times 10^{-7}\,\mu\Omega\,cm/Oe$ in the $Co_x(SiO_2)_{1-x}$ sample with $x = 1.0$ to $-3.8 \times 10^{-5}\,\mu\Omega\,cm/Oe$ in the sample with $x = 0.52$ (a factor of around 60). On the other hand, it was found that ρ_{xys} increases by a factor of approximately 1500 (from 0.067 to $96.2\,\mu\Omega\,cm$), indicating that the enhancement of the EHE is much stronger than the ordinary one. In the $Ni_x(SiO_2)_{1-x}$ samples, the ordinary Hall effect was found to increase by a factor of 120, while ρ_{xys} increased by a factor of approximately 750. The observed ratios of the extraordinary to ordinary contributions are in line with earlier observations for Co–SiO_2 [11] and NiFe–SiO_2 granular films [12].

The absolute enhancements of the Hall resistivities observed previously in $Co_x(SiO_2)_{1-x}$ samples were smaller (~ 190 for ρ_{xys} and 14 for ρ_{xyo}) [11], with the largest value of ρ_{xys} of $11.72\,\mu\Omega\,cm$. A more complete set of samples is now available, with more samples in the MIT region, and therefore we were able to measure more precisely samples very close to the transition.

This huge increase of both components of Hall resistivity in the vicinity of the MIT has been known as GHE [7]. Fig. 3 shows the values of ρ_{xx}, ρ_{xys}, and ρ_{xyo} as functions of x for $Co_x(SiO_2)_{1-x}$ (Fig. 3(a)) and $Ni_x(SiO_2)_{1-x}$ samples (Fig. 3(b)) at 5 K. It can be clearly seen that when x becomes close to $x_c \sim 0.5$, all the quantities are strongly enhanced.

It is worth noting that both the values of ρ_{xys} and ρ_{xyo} increase up to a value of x ($x = 0.52$ for Co and $x = 0.57$ for Ni), and then decrease again with decreasing x. This is also shown in Fig. 2. The samples where the maximum values of Hall effect are observed in both systems are exactly the ones that display a perfect $\rho \propto -\log T$ behavior, as shown in Fig. 1. For samples with lower x the temperature dependence of R is stronger than that, and can be well described by an $\exp[(T_0/T)^n]$ law

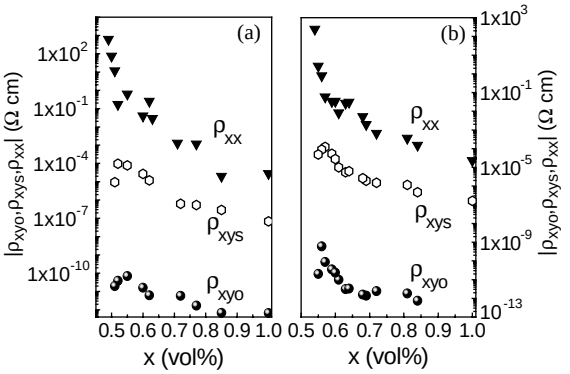

Fig. 3. Resistivity (▼), extraordinary Hall resistivity (○) and ordinary Hall resistivity (●) as functions of metal volume fractions x for: (a) $Co_x(SiO_2)_{1-x}$ and (b) $Ni_x(SiO_2)_{1-x}$ samples at $T = 5\,K$.

in some samples, that is a signature of hopping or tunneling.

Due to the uncertainty of determination of the MIT, different interpretations of the origin of GHE have been given in the literature. In the early experimental papers on GHE, it was assumed that the $\rho \propto -\log T$ behavior was a signature of weak localization [9]. However, a theory of (ordinary) GHE based on quantum interference in a metallic network has been recently developed [13], and it suggests that a maximum in Hall resistivity occurs at a composition higher than the classical percolation threshold, at a quantum percolation threshold. Experiments where such a maximum was observed in Cu–SiO_2 system were interpreted based on this theory [13]. However, some other observations [11,14] lead to another proposal, which indicates the largest GHE should be observed below the percolation threshold, in a tunneling regime. Note that magnetoresistance of a magnetic metal–insulator system has a maximum in a tunneling regime [5,6].

A structure with extremely fine dispersion of metal particles embedded in an insulating matrix is observed near the critical concentration, as shown in Fig. 4 for a $Ni_{0.6}(SiO_2)_{0.4}$ sample, and therefore such nanostructure is associated with the appearance of GHE. It was experimentally shown that annealing of the granular film leads to increase of the average particle size, and therefore to a decrease of the EHE (and magnetoresistance) [15].

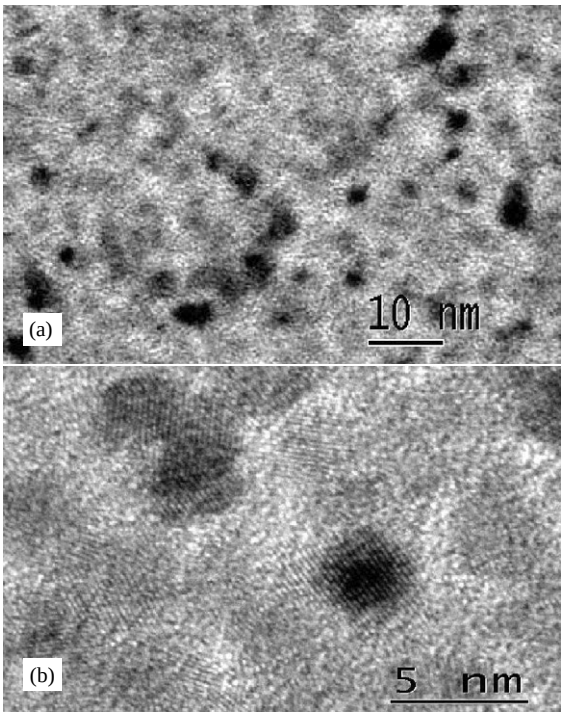

Fig. 4. (a) TEM image of $Ni_{0.60}(SiO_2)_{0.40}$ film. (b) High-resolution TEM image of the same sample, where nanometric Ni particles are clearly seen.

From the point of view of microscopic conduction mechanisms, MIT means a crossover from metallic conductivity with weak localization to tunneling, or hopping between separate granules across insulating barriers. In such framework, it is believed that GHE for polarized electrons is due to a combination of two effects: quantum interference and spin–orbit interactions. The total enhancement of the EHE may then be a product of the two terms that result from these two physical mechanisms. However, a complete picture of this interesting phenomenon is far from being complete, and this question will require thorough theoretical and experimental investigations.

3. EHE as a tool

Although the Hall effect in granular nanocomposites is not yet fully understood, it can be already employed as a powerful tool in the investigation of such materials. Magnetic percolation is also interrupted near the MIT, leading to superparamagnetic behavior of the composite and blocking phenomena at low temperatures. In bulk or thin film metallic samples the extraordinary Hall resistivity is directly proportional to the total magnetization, due to side jumps or skew scattering [17]. Deviations from this law in bimetal magnetic granular alloys are discussed in Ref. [16]. Comparison of Hall measurements with the magnetic results leads to new possibilities in understanding both the electronic and magnetic properties of granular nanocomposites.

In this section we show an example of how this effect can be explored as a tool to investigate magnetic properties, in the case of magnetic metal–insulator systems near the percolation threshold. In order to compare the temperature dependencies of magnetization and the extraordinary Hall coefficient in the composites near the critical concentration, we have measured zero-field-cooled (ZFC) and field-cooled (FC) magnetization curves on both Co–SiO_2 and Ni–SiO_2 samples.

Fig. 5 shows the ZFC/FC measurements of susceptibility on $Ni_x(SiO_2)_{1-x}$ (Figs. 5(a)–(c)) and $Co_x(SiO_2)_{1-x}$ (Fig. 5(d)) films near the MIT. The maximum of ZFC curves of the Ni–SiO_2 samples (Figs. 5(a)–(c)), related to the median blocking temperature (T_B), shifts towards higher temperatures when the concentration is increased, reflecting a continuous increase in the average grain size and interactions [18]. These samples are close to MIT, and show GHE, as seen in Fig. 2, with the largest value of EHE for sample with $x = 0.57$. For Co–SiO_2 sample ($x = 0.52$) the median T_B is close to room temperature. This sample is also close to MIT, with the largest EHE observed for Co–SiO_2 samples. A possible explanation for the smaller T_B observed in Ni/SiO_2 samples comes from the structural analysis made by TEM and X-ray diffraction studies [10], which indicate that the average grain size observed for Ni–SiO_2 samples is consistently smaller than the one for Co–SiO_2 films.

Fig. 6(a) shows the results of ZFC and FC measurements of both the magnetization M (open symbols) and the Hall resistivity $\rho_{xy} = (tU_{xy})/(I_{xx})$, where t is the thickness of sample,

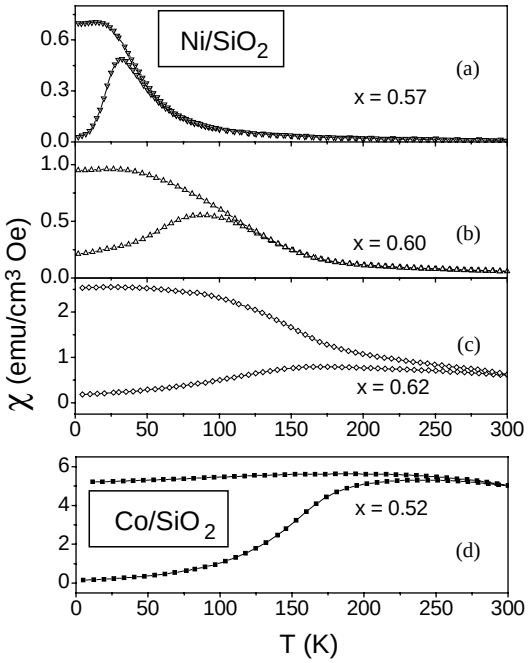

Fig. 5. ZFC and FC DC magnetic susceptibility, measured at 20 Oe for granular $Ni_x(SiO_2)_{1-x}$ films with (a) $x = 0.57$, (b) 0.60, (c) 0.62, and (d) for $Co_x(SiO_2)_{1-x}$ with $x = 0.52$.

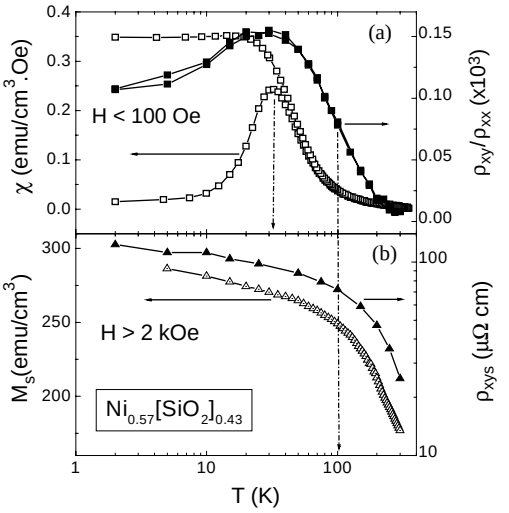

Fig. 6. (a) ZFC and FC DC magnetic susceptibility (open symbols) and ZFC/FC Hall resistivity (filled symbols) measured at 60 Oe for granular $Ni_x(SiO_2)_{1-x}$ film with $x = 0.57$. (b) Saturation magnetization (open symbols) and extraordinary Hall resistivity (filled symbols) measured at 2 T for the same sample.

U_{xy} the Hall voltage, and I_{xx} is the longitudinal current, for Ni–SiO_2 sample with $x = 0.57$. Both the M vs. T and ρ_{xy} vs. T ZFC curves have maxima. One can associate the positions of the maxima with the blocking temperature [18]. However, the FC curves are different in the two measurements. In the EHE curve, no difference between ZFC and FC is detected. The extraordinary Hall resistivity is usually assumed to be proportional to magnetization and a power of resistivity: $\rho_{xys} \propto M_z \rho_{xx}^n$, where n depends on the EHE mechanism [8].

From the data shown in Fig. 6, it follows that no such simple correlations are observed in this granular system. In a metal–insulator composite, only those electrons traveling in conduction critical paths can contribute to the Hall signal, thus only magnetization of the material belonging to these paths is important in the Hall measurements. Despite the differences in the magnetic and transport ZFC/FC curves, one can see that the peak in the curves occurs roughly at the same temperature, indicating a clear-cut correlation between the two properties. In Fig. 6(b) the comparison between the saturation magnetization M_s and the extraordinary Hall resistivity ρ_{xys} is shown, both measured at fields larger than 2 T. As the temperature increases, more and more particles are free to rotate, and this is reflected by a drop of M_s and by an even stronger drop of the value of ρ_{xys}.

It is generally difficult to measure EHE at such low metallic concentrations, and apparently this was why we could not observe noticeable differences between ZFC and FC curves in the EHE measurement. We checked these ideas on Co–Ag system, where resistance is much lower, and an excellent confirmation of this difference was found. Figs. 7(a)–(c) show the result of ZFC and FC measurements of both the magnetization M (open symbols) and the Hall resistivity ρ_{xy}/R (filled symbols), for Co_xAg_{1-x} samples with $x =$ 0.10, 0.15 and 0.25, in a field of 200 Oe. The ratio ρ_{xy}/R is supposed to be proportional to M, assuming a skew scattering mechanism for EHE in magnetic granular alloys [19]. Both the M vs. T

and ρ_{xy}/R vs. T ZFC curves display maxima, which are not reproduced in the FC measurements. In this case T_b can also be obtained from the Hall measurements. For the sample with $x = 0.10$, both EHE and magnetization curves have the maxima at the same temperature $T_b = 20\,K$. However, as seen in Figs. 7(b) and (c), no such simple correlation is observed at higher concentrations. The positions of the maxima of EHE are shifted to lower temperatures compared to the magnetization curves for $x = 0.15$ (Fig. 7(b)) and $x = 0.25$ (Fig. 7(c)), and the difference is larger for the samples with higher Co concentrations.

This result can be explained by the correlation between the EHE and particle size distributions [15]. While the magnetization is given by the total contribution of the magnetic moment of each magnetic grain, weighted by the corresponding distribution function, the Hall effect is more sensitive to the smaller particles of the system [16,19]. This fact must be taken into account if one wants to use the EHE as a research tool, to investigate magnetization of diluted systems when conventional magnetic measurements are not sensitive enough or when they are not available. However, this interesting dependence on the smaller particles of the system can be positively explored to perform size selective measurements, in order to study TMR, magnetic interactions and spin-dependent transport in such complex nanostructures.

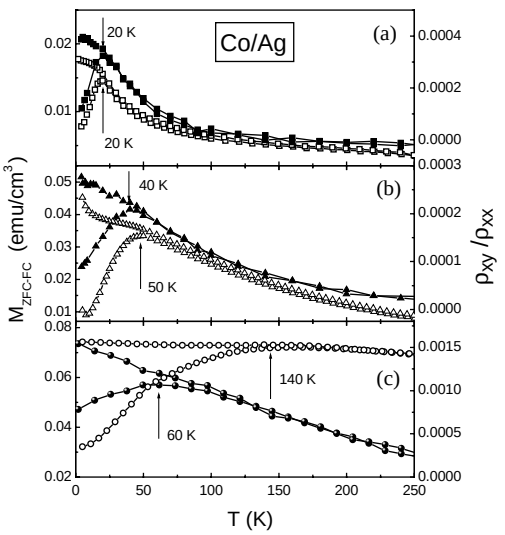

Fig. 7. ZFC and FC magnetization (open symbols) and Hall resistivity (filled symbols) for Co_xAg_{1-x} samples with (a) $x = 0.10$, (b) $x = 0.15$ and (c) $x = 0.25$, in a field of 200 Oe.

4. Conclusion

In this paper we presented a review of the giant Hall effect, with emphasis on novel experimental data obtained in Ni–SiO_2, Co–SiO_2 and Co–Ag films prepared by co-sputtering. Maximum GHE values were observed in samples that display a $\rho \propto -\log T$ behavior, that is usually attributed to weak localization or electron–electron interaction effects in a disordered metallic system. However, it is clear that systematic studies (both theoretical and experimental) are still necessary to clarify several aspects of the phenomenon, in order to achieve a complete understanding of the physical mechanisms behind this intriguing effect that occurs in the vicinity of the MIT of granular nanostructures.

Although not yet fully understood, the Hall effect in granular systems is very sensitive to the details of the microstructure, and therefore, it can be used as an additional tool to investigate the blocking phenomenon and superparamagnetism in granular magnetic systems. An example on Ni–SiO_2 and Co_xAg_{1-x} films was shown, by comparing zero-field-cooled (ZFC) and field-cooled (FC) EHE measurements in a small field with the corresponding measurements with conventional magnetometry. Although the EHE measurements correlate with the overall magnetization of the system, the results may differ from the ones obtained through conventional magnetometry, because the transport measurements are more sensitive to the smaller particles of the system. This fact must be taken into account when this kind of investigation is performed, but it can be extremely useful for highly sensitive measurements, for example, when the magnetic signal is too small to be detected by usual magnetic methods, or when a SQUID magnetometer is not available.

Acknowledgements

TEM studies were performed at the Laboratório de Microscopia Eletrônica (LME–LNLS), Campinas, Brazil. This work was financially supported by FAPESP and CNPq (Brazilian agencies). X.X.Z. acknowledges the support from Hong Kong RGC Grant (HKUST 6159/99P). A.B.P. was partially supported at University of Washington by the Campbell Endowment.

References

[1] B. Abeles, P. Sheng, M.D. Coutts, Y. Arie, Adv. Phys. 24 (1975) 40.
[2] P. Sheng, Philos. Mag. B 65 (1992) 357.
[3] M.C. Chan, A.B. Pakhomov, Z.-Q. Zhang, J. Appl. Phys. 87 (2000) 1584;
E.Z. Luo, A.B. Pakhomov, Z.-Q. Zhang, M.C. Chan, I.H. Wilson, J.B. Xu, X. Yan, Physica B 279 (2000) 98.
[4] J.I. Gittleman, Y. Goldstein, S. Bozowski, Phys. Rev. B 5 (1972) 3609;
S. Helman, B. Abeles, Phys. Rev. Lett. 37 (1976) 1429.
[5] H. Fujimori, S. Mitani, S. Ohnuma, Mater. Sci. Eng. B 31 (1995) 219.
[6] A. Milner, A. Gerber, B. Groisman, M. Karpovsky, A. Gladkikh, Phys. Rev. Lett. 76 (1996) 475.
[7] A.B. Pakhomov, X. Yan, B. Zhao, Appl. Phys. Lett. 67 (1995) 3497.
[8] C.M. Hurd, The Hall Effect in Metals and Alloys, Plenum Press, New York, 1972;
A. Fert, D.K. Lottis, in: J. Evetts (Ed.), Concise Encyclopedia of Magnetic and Superconducting Materials, Pergamon, Oxford, NY, 1992, p. 287.
[9] A.B. Pakhomov, X. Yan, Solid State Commun. 99 (1996) 139.
[10] L.M. Socolovsky, J.C. Denardin, A.L. Brandl, M. Knobel, X.X. Zhang, J. Magn. Magn. Mater. 262 (2003) 102, these proceedings.
[11] J.C. Denardin, A.B. Pakhomov, M. Knobel, H. Liu, X.X. Zhang, J. Phys.: Condens. Matter 12 (2000) 3397;
J.C. Denardin, A.B. Pakhomov, M. Knobel, H. Liu, X.X. Zhang, J. Magn. Magn. Mater. 226–230 (2001) 680.
[12] A.B. Pakhomov, X. Yan, N. Wang, X.N. Jing, B. Zhao, K.K. Fung, J. Xhie, T.F. Hung, S.K. Wong, Physica A 241 (1998) 344.
[13] X.X. Zhang, C.C. Wan, H. Liu, Z.Q. Li, P. Sheng, J.J. Lin, Phys. Rev. Lett. 86 (2001) 5562;
C.C. Wan, P. Sheng, Phys. Rev. B 66 (2002) 075309.
[14] B.A. Aronzon, V.V. Rylkov, D.Y. Kovalev, E.Z. Meilikhov, A.N. Lagarkov, M.A. Sedova, M. Goiran, N. Negre, B. Raquet, Phys. Stat. Sol. 218 (2000) 169;
B.A. Aronzon, A.B. Granovskii, D.Y. Kovalev, E.Z. Meilikhov, V.V. Ryl'kov, M.V. Sedova, JETP Lett. 71 (2000) 469.
[15] X.N. Jing, N. Wang, A.B. Pakhomov, K.K. Fung, X. Yan, Phys. Rev. B 53 (1996) 14032.
[16] J.C. Denardin, A.B. Pakhomov, A.L. Brandl, L.M. Socolovsky, M. Knobel, X.X. Zhang, Appl. Phys. Lett. 82 (2003) 763.
[17] A. Gerber, A. Milner, J. Tuaillon-Combes, M. Négrier, O. Boisron, P. Mélinon, A. Perez, J. Magn. Magn. Mater. 241 (2002) 340.
[18] J.C. Denardin, A.L. Brandl, M. Knobel, P. Panissod, A.B. Pakhomov, H. Liu, X.X. Zhang, Phys. Rev. B 65 (2002) 064422.
[19] A. Vedyaev, A. Granovsky, A. Kalitsov, F. Brouers, JETP 85 (1997) 1204.